OFFICE OF NAVAL RESEARCH

GRANT: N00014-93-0545

R & T CODE: 413V005

Technical report # 6

THE HYDROPHOBIC ELECTRODE

by

B. Kurtyka and R. de Levie

prepared for publication in the
Journal of Electroanalytical Chemistry

Chemistry Department, Georgetown
University, Washington DC 20057

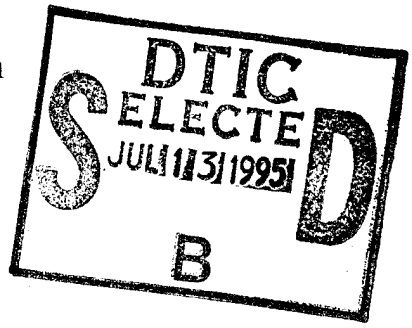

June 26, 1995

REPORT DOCUMENTATION PAGE

Form Approved
OMB No. 0704-0188

1. AGENCY USE ONLY (*Leave blank*)	2. REPORT DATE	3. REPORT TYPE AND DATES COVERED
	June 26, 1995	Technical

4. TITLE AND SUBTITLE

THE HYDROPHOBIC ELECTRODE

5. FUNDING NUMBERS

N00014-93-1-0545

6. AUTHOR(S)

B. Kurtyka and R. de Levie

7. PERFORMING ORGANIZATION NAME(S) AND ADDRESS(ES)

Chemistry Department, Georgetown University, Washington DC

8. PERFORMING ORGANIZATION REPORT NUMBER

Technical report #6

9. SPONSORING/MONITORING AGENCY NAME(S) AND ADDRESS(ES)

Office of Naval Research, Dept. of the Navy, Arlington VA 22217

10. SPONSORING/MONITORING AGENCY REPORT NUMBER

11. SUPPLEMENTAL NOTES

12a. DISTRIBUTION AVAILABILITY STATEMENT

Approved for public release; distribution unlimited

12b. DISTRIBUTION CODE

13. ABSTRACT (*Maximum 200 words*)

Condensed adsorbate monolayers ("compact films") formed by either salts or neutral adsorbates can provide a hydrophobic micro-environment around the electrode, even when this electrode is immersed in an aqueous solution. In such a micro-environment, reaction mechanisms can be altered. Specifically, the absence of interfacial water may prevent protonation of anion radicals formed by electron transfer, so that mechanisms involving dimerization may be favored. Condensed adsorbate films then allow the use of aqueous solvents for electrochemical syntheses where, otherwise, more expensive and environmentally more troublesome aprotic solvents might be needed. The precise reaction mechanism depends on the adsorbate used, thus providing the experimentalist with a further tool to steer the reaction pathway.

14. SUBJECT TERMS

Two-dimensional condensation
Fumarodinitrile hydrodimerization

15. NUMBER OF PAGES

17

16. PRICE CODE

17. SECURITY CLASSIFICATION OF REPORT	18. SECURITY CLASSIFICATION OF THIS PAGE	18. SECURITY CLASSIFICATION OF ABSTRACT	20. LIMITATION OF ABSTRACT
Unclassified	Unclassified	Unclassified	Unlimited

THE HYDROPHOBIC ELECTRODE

Bogdan Kurtyka and Robert de Levie, Chemistry Department
Georgetown University, Washington DC 20057 USA

The electrochemical reduction of olefins is believed to start with the transfer of an electron, generating a radical anion. When the resulting radical anion is not stable, subsequent reactions often produce a mixture of final reaction products. The relative yields of these products depend on the nature of the reagent as well as on that of the solvent. For 'diactivated' unsaturated olefins (in which the double bond has for neighbors two 'activating' electron-withdrawing groups) such as fumarodinitrile, *trans* N≡C–CH=CH–C≡N, the dominant reaction pathway can be manipulated by changing the nature of the metal-solution interface. It is the purpose of this communication to illustrate such behavior.

Fumarodinitrile was chosen for the present study because its reduction at the mercury-water interface occurs at a relatively positive potential, where double layer properties can be measured and modified conveniently. Its reduction leads to two main products: succinodinitrile results from the uptake of two electrons and two protons, thereby reducing the central double bond of fumarodinitrile, while one-electron reduction followed by dimerization produces 1,2,3,4-tetracyanobutane. Mercury and aqueous electrolyte solutions were selected because of the large amount of interfacial knowledge already available for this combination. Polarography is a convenient method because the height of the limiting current clearly indicates the nature of the electrode process: reduction to the saturated monomer is accompanied by the uptake of two electrons per molecule of reagent, whereas electrodimerization involves two electrons and two protons per *two* reagent molecules, and therefore registers as a one-electron wave.

Fig. 1 shows the interfacial capacitance as a function of potential for 0.5 M aqueous NaBr in the presence and absence of 1 mM tetrabutylammonium bromide, and Fig. 2 the polarographic reduction of 0.1 mM fumarodinitrile in those solutions. In the presence of tetrabutylammonium bromide, the approximately two-electron wave of the reduction of fumarodinitrile to succinodinitrile is replaced by a one-electron wave at those potentials where the interfacial capacitance is strongly depressed because of the presence of a condensed interfacial film [1,2]. The transition from one dominant mechanistic pathway to the other occurs precisely at the potential where the capacitance-potential plot locates the transition associated with the dissolution of the condensed film, and in fact traces it faithfully as the tetrabutylammonium concentration is changed.

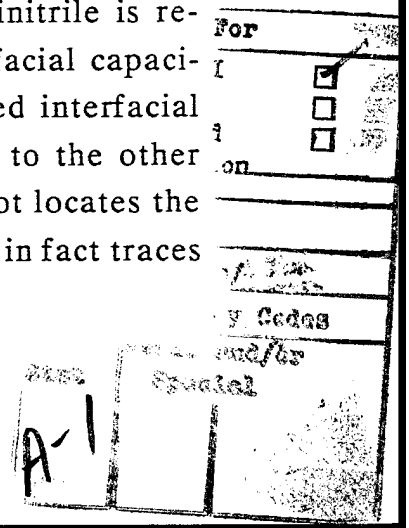

Figs. 1,2

When the supporting electrolyte itself is strongly adsorbed, as in the case of potassium 1S-(+)-10-camphorsulfonate, the experiment can be performed in the absence of an additional electrolyte. Again, a pronounced change in the polarographic wave occurs at the potential where, according to the capacitance, the condensed film dissolves, as can be seen in Figs. 3 and 4.

Figs. 3,4

Figs. 5 and 6 show similar results in aqueous 0.5 M NaF in the absence and presence of 2,3-dimethylpyridine. Again, the polarograms exhibit a dramatic change from a one-electron reduction to a two-electron wave at the potential where the condensed film of 2,3-dimethylpyridine dissolves.

Figs. 5,6

The situation is somewhat more complicated in the presence of adenosine, see Figs. 7 through 9. 'Normal' adenosine adsorption (at potentials negative of the condensed region, or at lower adenosine concentrations where no interfacial condensation occurs) has no appreciable effect on the polarographic wave of fumarodinitrile, while formation of a capacitance pit leads to a change from a two-electron to a one-electron wave, see Fig. 8. In this case, however, the polarographic transition from one reduction mechanism to the other does not appear to be quite as sharp. This is not surprising since the interfacial capacitance has a prominent hysteresis loop, indicating that the formation of the condensed film is a kinetically hindered process.

Figs. 7,8

That the kinetics of film formation are indeed the reason for this behavior can be gauged from Fig. 9, where we show the time-dependence of the capacitance in the absence of fumarodinitrile, and the corresponding current-time curves for the reduction of fumarodinitrile under otherwise identical conditions. The capacitance-time curves clearly document the rate of formation of the condensed adenosine film as a function of the applied potential. The current-time-curves in the presence of fumarodinitrile indicate that the current switches from a two-electron process to a one-electron reduction with the very same time constant as that of the formation of the condensed film. The capacitance-potential curves in Fig. 7 were measured on hanging mercury droplets, and therefore do not show as clearly this interplay between drop time and slow film formation.

Fig. 9

Incidentally, one may note a rather regular oscillation on the current-time curves of Fig. 9b. This is an instrumental artifact, resulting from interference between the mains frequency and the rate at which the current is sampled. In the present example, the data were sampled at an acquisition rate of $66^{2}/_{3}$ Hz, which when combined with noise at the power-line frequency of 60 Hz caused a beat frequency of $6^{2}/_{3}$ Hz. One can easily avoid such oscillations by more careful selection of the sampling frequency; we here purposely illustrate this artifact of digital data acquisition because its purely instrumental nature has not always been recognized [3].

While the above data show that adsorbate condensation can alter the dominant reduction pathway, it does not mean that condensation is always required. For example, the presence of a coumarin pit almost completely suppresses the reduction wave, while coumarin adsorption at potentials past the negative pit edge leads to a one-electron wave. Again, the pit edge is not sharp in the polarogram because pit formation and drop growth have comparable time constants.

All our data are consistent with the notion that fumarodinitrile dimerization is favored in the absence of interfacial water. The formation of a capacitance pit, either by a salt (as in Figs. 1 and 3) or by a neutral adsorbate (as in Figs. 5 and 7), is believed to be accompanied by the expulsion of water from the interface; the strong adsorption of coumarin at potentials negative of its pit may well have a similar effect.

While the present examples vividly illustrate this effect, we are by no means the first to draw attention to it. For example, Puglisi et al. [4] showed that the products of the electroreductive coupling of benzaldehyde to hydrobenzoin changed dramatically in the presence of tetrabutylammonium ions. Likewise, Kastening & Kazemifard [5] and Gierst [6] invoked the absence of interfacial water in the apparent stability of superoxide ions in the presence of triphenylphosphine oxide and quinoline, both of which are now known to form condensed adsorbate films. Damaskin [7] assumed that water was excluded from a condensed guanidinium nitrate film, and Guidelli et al. [8-10] postulated that interfacial water is more effective in protonating radical anions than bulk water, and that this is the reason for the enhanced dimerization yield in the presence of strong adsorbates.

It appears that, in all the above examples, we have an electrode which presents a hydrophobic micro-environment to the faradaic process even though it is surrounded by an aqueous phase. Such a hydrophobic environment can be maintained effectively by the self-association of adsorbed hydrophobic molecules, which maintain a pinhole-free, self-repairing monolayer as long as the bulk concentration of the adsorbate is high enough to support the condensed film. (Since the adsorbate is not consumed, this requirement is easily satisfied.) Apparently, a similar mechanism acts in the hydrodimerization of acrylonitrile to adiponitrile [11].

Finally we briefly describe the most plausible reaction mechanisms in some of the above-described examples, consistent with a comparison of extensive polarographic and cyclic-voltammetric measurements with the classification of Nadjo & Savéant [12].

In general, in the presence of a condensed film, the first reaction is the transfer of a single electron to generate the anion radical,

$$R + e^- \rightarrow R^{\cdot -} \qquad (1)$$

When the interface is covered with a condensed tetrabutylammonium monolayer, reaction (1) is fast, and the rate-limiting process is the subsequent radical-radical coupling,

$$R^{\cdot -} + R^{\cdot -} \rightarrow R_2^{2-} \qquad (2a)$$

In the presence of a condensed film of 2,3-dimethylpyridine in strongly basic solution, the process proceeds through radical-substrate coupling (2b) followed by a second electron transfer,

$$R^{\cdot -} + R \rightarrow R_2^{\cdot -} \qquad (2b)$$

$$R_2^{\cdot -} + e^- \rightarrow R_2^{2-} \qquad (3b)$$

while the most likely mechanism in 2,3-dimethylpyridine film in borate buffer is ion-pairing between the anion radical and the protonated form of pyridine, followed by reaction with another anion radical,

$$R^{\cdot -} + HPy^+ \rightarrow RHPy^{\cdot} \qquad (2c)$$

$$RHPy^{\cdot} + R^- \rightarrow R_2H^- + Py \qquad (3c)$$

Finally, in the presence of a condensed 1S-(+)-10-camphorsulfonate monolayer, the electron transfer step (1) is slow, and hence no further information regarding the mechanism is obtainable.

Identification of the main reaction product is feasible by isolating the reaction product and subsequent examination by proton magnetic resonance. In deuteroacetonitrile, succinodinitrile exhibits a single peak, whereas the dimer exhibits two complex spectral features, around 3.00 and 3.54 ppm, with the characteristics of virtual coupling, see Fig. 10. The interpretation of such a spectrum is complicated by the possible presence of meso and d,l-isomers, and by the complexity of AA'BB'CC' spin systems [13,14], and was not attempted.

Fig. 10

Note that the chemical reactions are supposed to proceed in the solution adjacent to the electrode rather than in the interfacial film. In agreement with this, no enhanced optical activity of the final reaction product was observed when fumarodinitrile was reduced in the presence of a condensed film of 1S-(+)-10-camphorsulfonate.

In summary, condensed adsorbate monolayers ("compact" films), formed by either salts or neutral adsorbates, can provide a hydrophobic micro-environment around the electrode, even when this electrode is immersed in an aqueous solution. In such a micro-environment, reaction mechanisms can be altered. Specifically, the absence of interfacial water may prevent protonation of anion radicals formed by electron transfer, so that mechanisms involving dimerization may be favored. Condensed adsorbate films then allow the use of aqueous solvents for electrochemical syntheses where, otherwise, more expensive and environmentally more troublesome aprotic solvents might be needed. The precise reaction mechanism depends on the adsorbate used, thus providing the experimentalist with a further tool to steer the reaction pathway.

Acknowledgement

We thank Prof. David K. Gosser Jr. of City University of New York for kindly making available to us his digital simulation program CVSim, of which we used a modified version to simulate cyclic voltammograms. We also thank Dr. Stephen Feldberg of Brookhaven National Laboratory for verifying some of our simulations on the more recent program DigiSim, and Dr. Edwin Becker and Dr. Herman J. C. Yeh of the National Institutes of Health for the 500 MHz proton magnetic resonance spectrum of Fig. 10. Financial support from the Office of Naval Research under grant N00014-93-1-0545 is gratefully acknowledged.

References

1. R. de Levie, Chem. Revs. 88 (1988) 599.
2. C. Buess-Herman, Adsorption of molecules at metal electrodes, J. Lipkowski & P. N. Ross, eds., VCH (1992) 77.
3. M. Schrettenbrunner, P. Chaiyasith, H. Baumgärtel & U. Retter, Ber. Bunsenges. 97 (1993) 847.
4. V. J. Puglisi, G. L. Clapper & D. H. Evans, Anal. Chem. 41 (1969) 279.
5. B. Kastening & G. Kazemifard, Ber. Bunsenges. 74 (1970) 551.
6. J. Chevalet, F. Rouelle, L. Gierst & J. P. Lambert, J. Electroanal. Chem. 39 (1972) 201.
7. S. L. Dyatkina, B. B. Damaskin & M. Z. Vygotskaya, Elektrokhim. 16 (1980) 996.
8. M. R. Moncelli, F. Pergola, G. Aloisi & R. Guidelli, J. Electroanal. Chem. 143 (1983) 233.
9. G. Piccardi, L. Nucci, F. Pergola & R. Guidelli, J. Electroanal. Chem. 164 (1984) 145.
10. M. R. Moncelli, R. Guidelli & M. Carla, J. Electroanal. Chem. 313 (1991) 313.
11. M. M. Baizer, J. Electrochem. Soc. 111 (1964) 215.
12. L. Nadjo & J. M. Savéant, J. Electroanal. Chem. 44 (1973) 327.
13. R. J. Abraham & J. R. Monasterios, J. Chem. Soc. Perkin II (1975) 699.
14. J. Beger, H. Schiefer, L. Schröder & A. Zschunke, J. Prakt. Chem. 322 (1980) 610.

Figure legends

Fig. 1. The interfacial capacitance of mercury in contact with aqueous 0.5 M NaBr with and without (broken line) 1 mM tetrabutylammonium bromide, recorded at 5°C with a frequency of 500 Hz, an amplitude of 5 mV and a sweep rate of -5 mV s^{-1}.

Fig. 2. The polarogram of aqueous 0.5 M NaBr + 0.1 mM fumarodinitrile with and without (broken line) 1 mM tetrabutylammonium bromide at 5°C, recorded with a sweep rate of -1 mV s^{-1}.

Fig. 3. The interfacial capacitance of mercury in contact with aqueous 0.3 M potassium 1S-(+)-10-camphorsulfonate, recorded at 5°C with a frequency of 500 Hz, an amplitude of 5 mV and a sweep rate of -5 mV s^{-1}.

Fig. 4. The polarogram of aqueous 0.3 M potassium 1S-(+)-10-camphorsulfonate + 0.1 mM fumarodinitrile at 5°C, recorded with a sweep rate of -1 mV s^{-1}.

Fig. 5. The interfacial capacitance of mercury in contact with aqueous 0.5 M NaF with and without (broken line) 4.8 mM 2,3-dimethylpyridine at 10°C, recorded with a frequency of 500 Hz, an amplitude of 5 mV and a sweep rate of -5 mV s^{-1}.

Fig. 6. The polarogram of aqueous 0.5 M NaF + 0.1 mM fumarodinitrile at with and without (broken line) 4.8 mM 2,3-dimethylpyridine at 10°C, recorded with a sweep rate of -1 mV s^{-1}.

Fig. 7. The interfacial capacitance of mercury in contact with aqueous 0.5 M NaF with and without (broken line) 5 mM adenosine at 5°C, recorded with a frequency of 500 Hz, an amplitude of 5 mV, and a sweep rate of -5 and +5 mV s^{-1} respectively, as indicated by arrows.

Fig. 8. The polarogram of aqueous 0.5 M NaF + 0.1 mM fumarodinitrile at with and without (broken line) 5 mM adenosine at 10°C, recorded with a sweep rate of -1 mV s^{-1}.

Fig. 9. (a): The interfacial capacitance of a growing mercury drop in contact with aqueous 0.5 M NaF + 5 mM adenosine at 10°C at three different potentials: (1): -1.40 V; (2) -1.47 V; and (3) -1.49 V, all vs. SCE.

(b): The corresponding polarographic current-time curves of 0.1 mM fumarodinitrile in aqeous 0.5 M NaF + 5 mM adenosine at 10°C at the same three potentials: (1): -1.40 V; (2) -1.47 V; and (3) -1.49 V, clearly showing that the time course of the two-dimensional adenosine condensation is faithfully reflected in that of the polarographic current for the fumarodinitrile reduction.

Fig. 10. The 500 MHz proton magnetic resonance spectrum, in deuterated acetonitrile, of the reaction product formed by exhaustive preparative electrolysis of fumarodinitrile from aqueous 0.5 M NaBr + 1 mM tetrabutylammonium bromide + 0.05 M fumarodinitrile at potentials within the region of stability of the condensed tetrabutylammonium film, and subsequently crystallized and dissolved in deuteroacetonitrile.

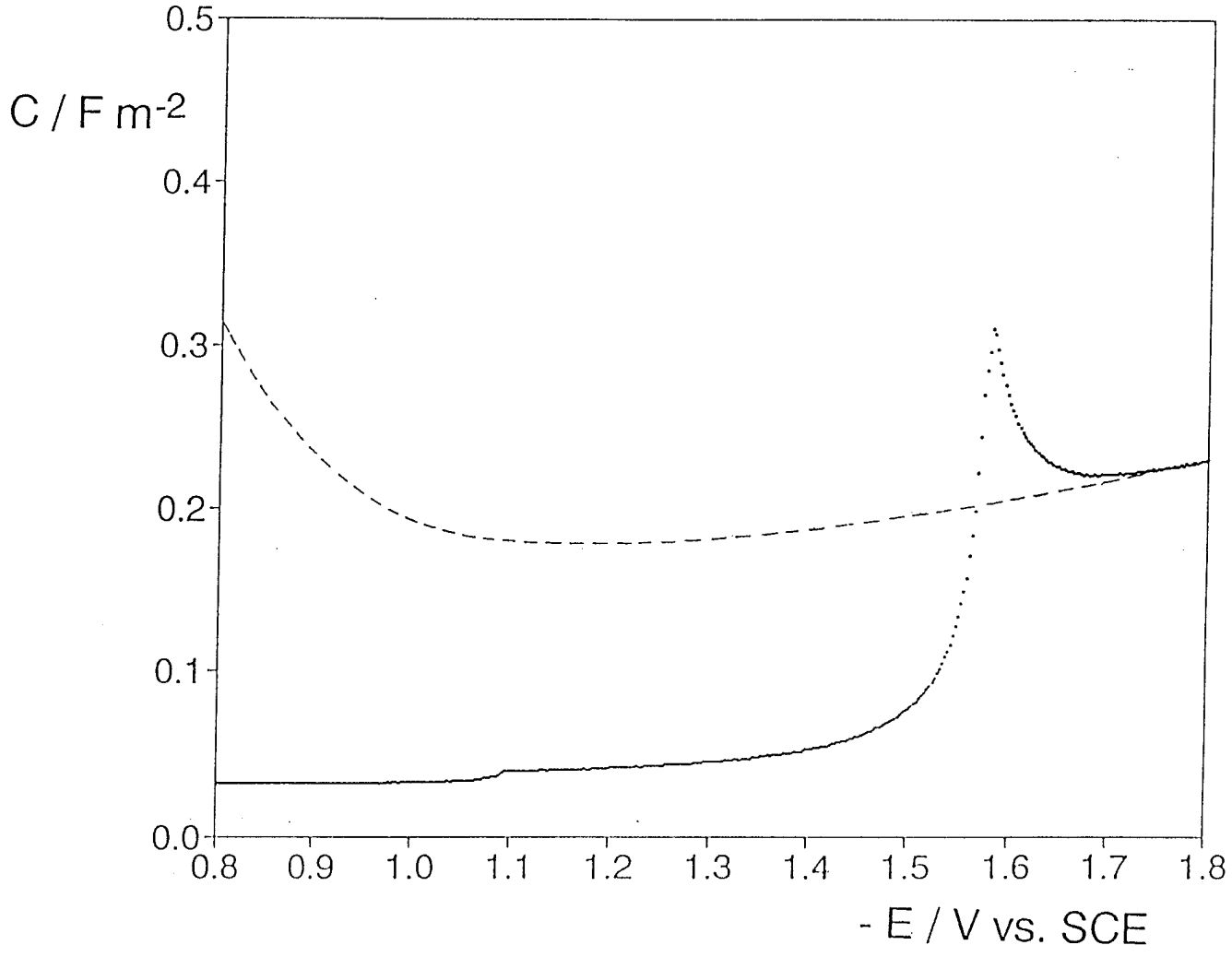

FIG. 1

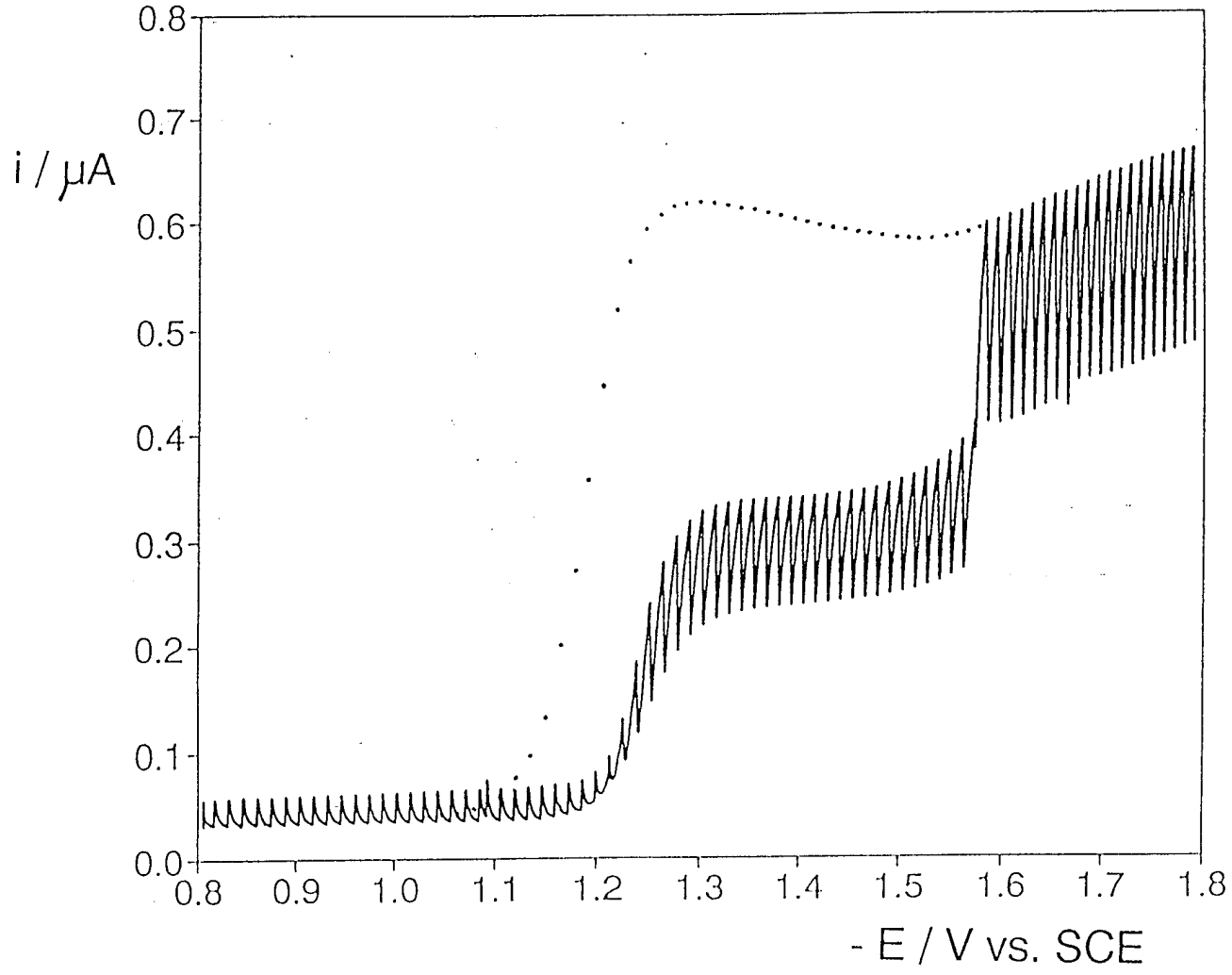
i / μA
0.8
0.7
0.6
0.5
0.4
0.3
0.2
0.1
0.0
0.8
0.9
1.0
1.1
1.2
1.3
1.4
1.5
1.6
1.7
1.8
- E / V vs. SCE

FIG. 2

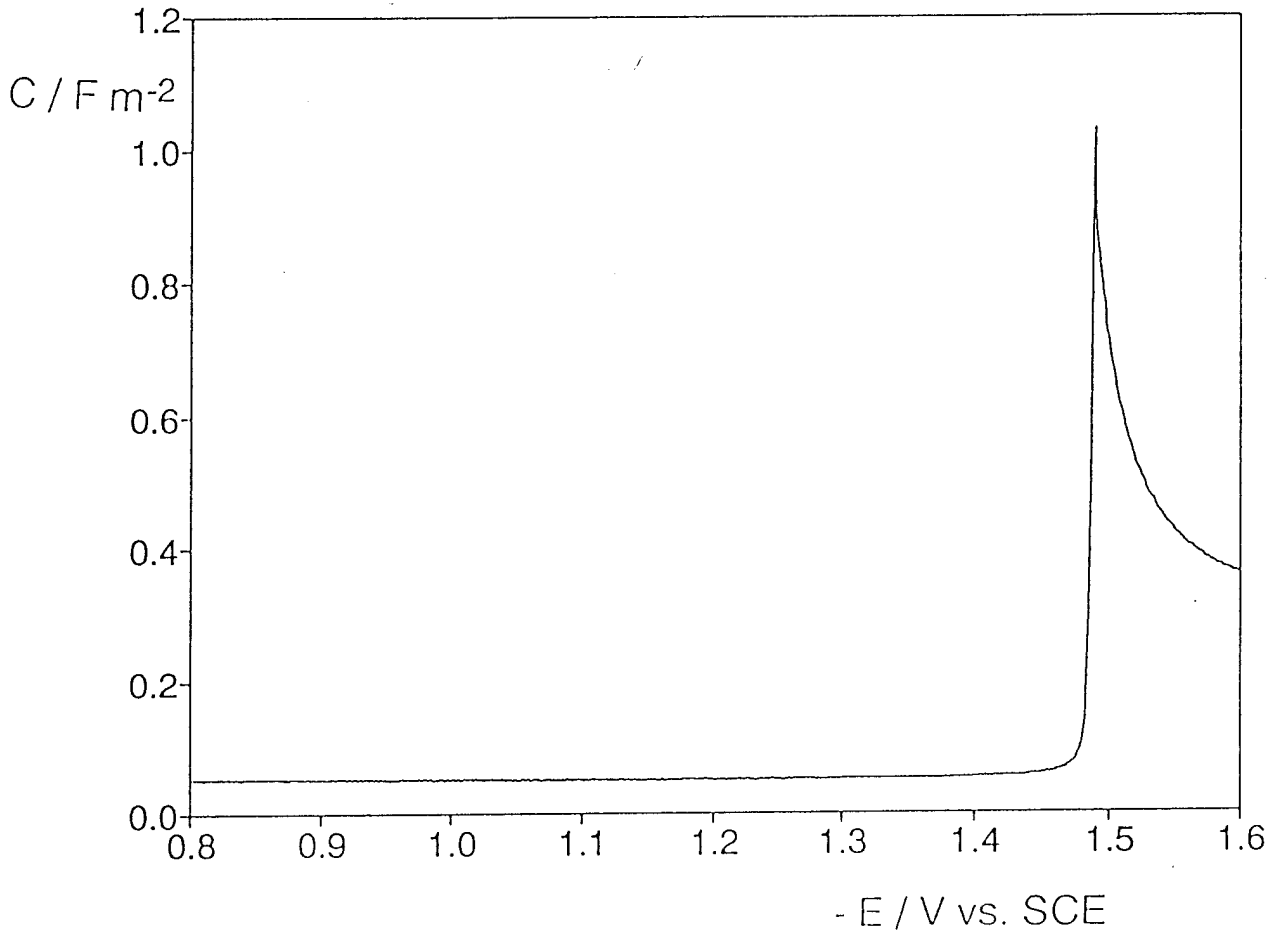

FIG. 3

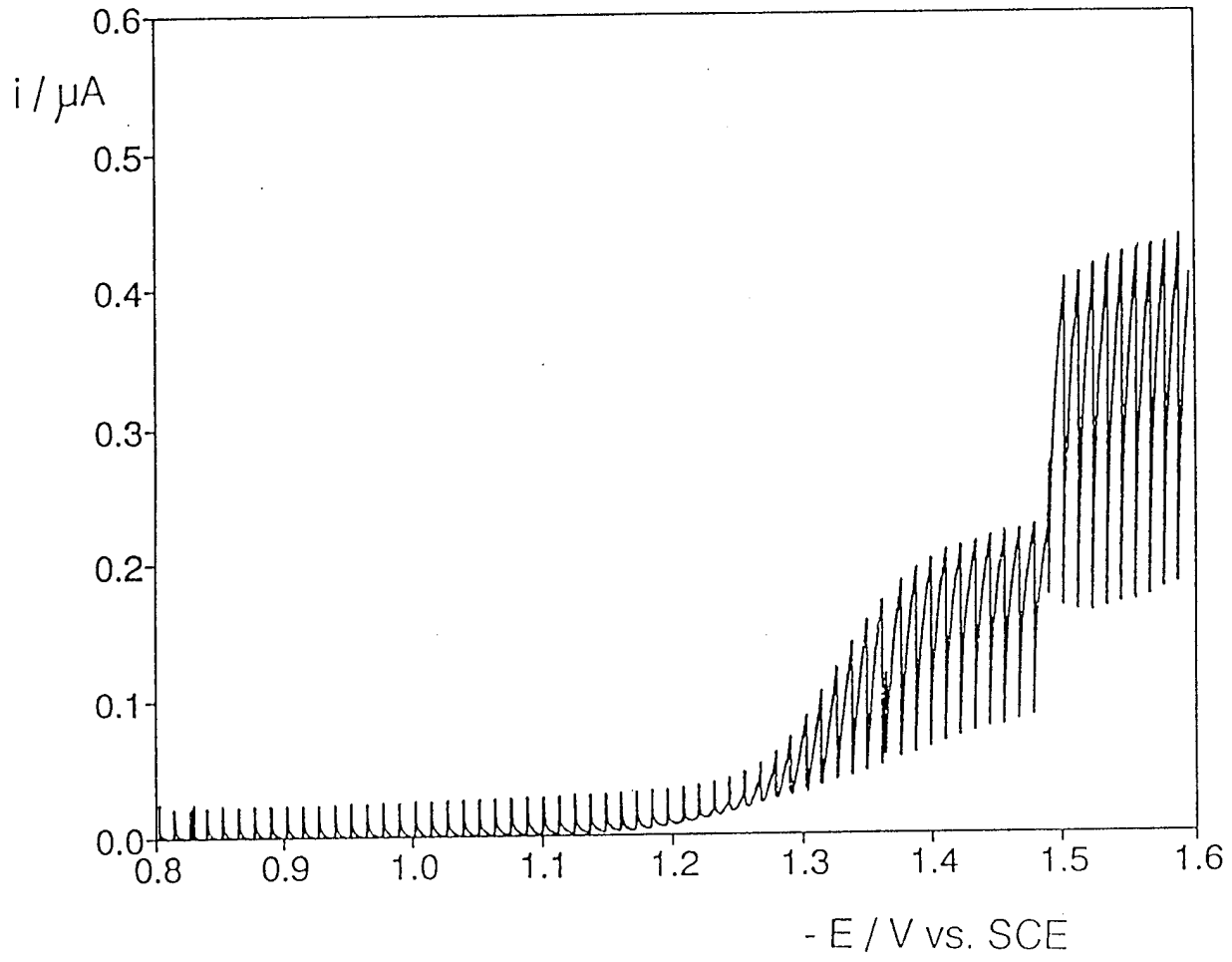

FIG. 4

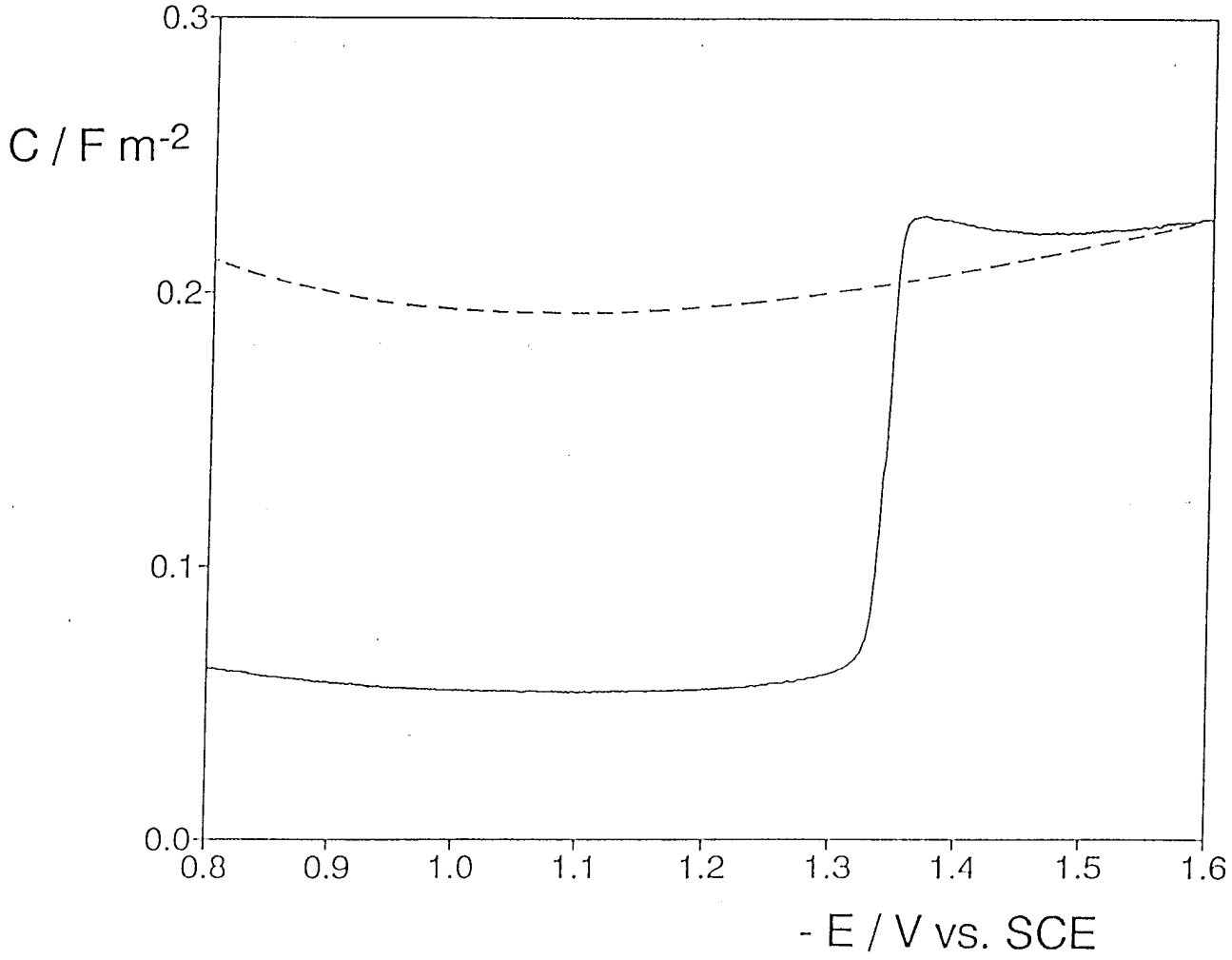

FIG 5

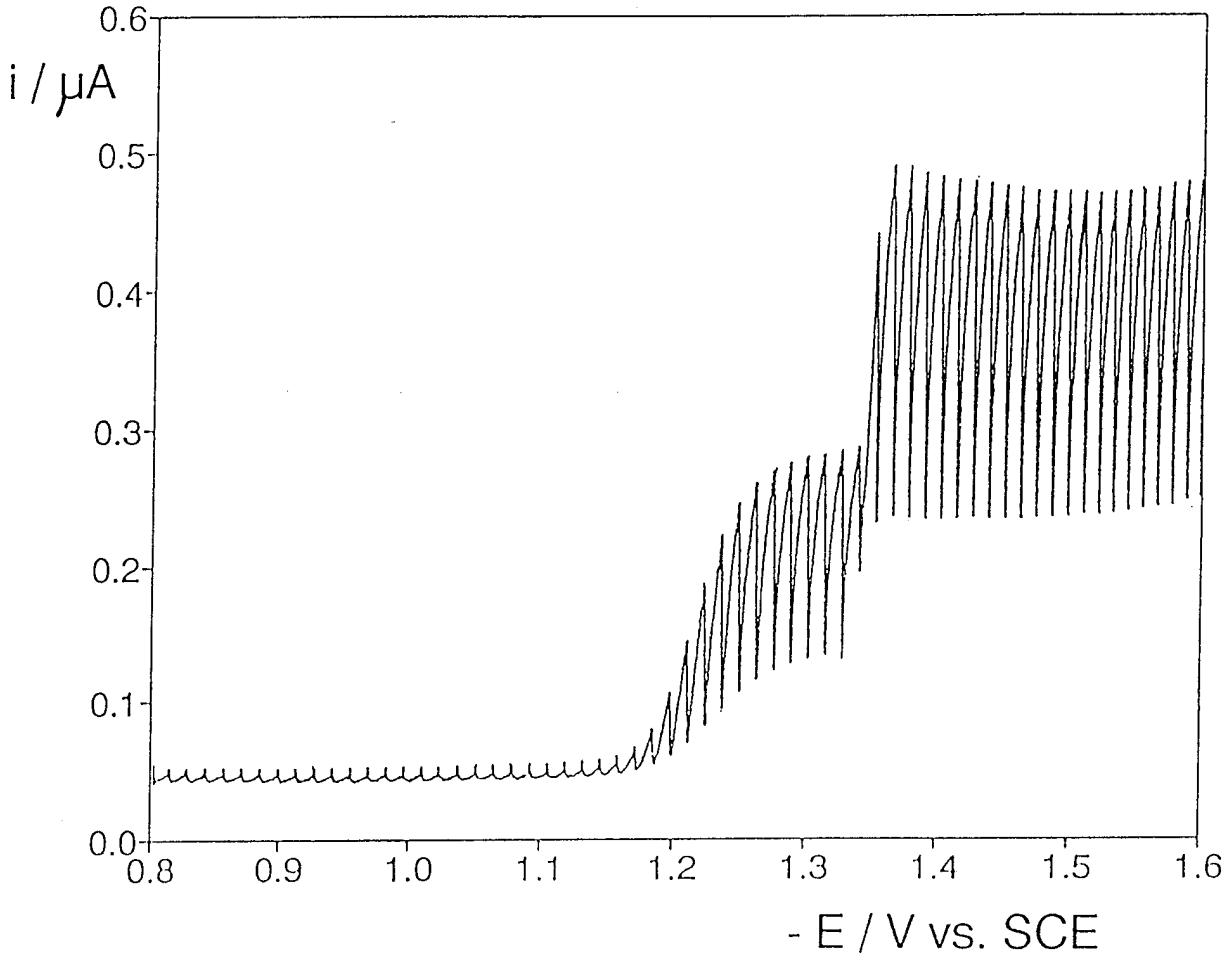

FIG. 6

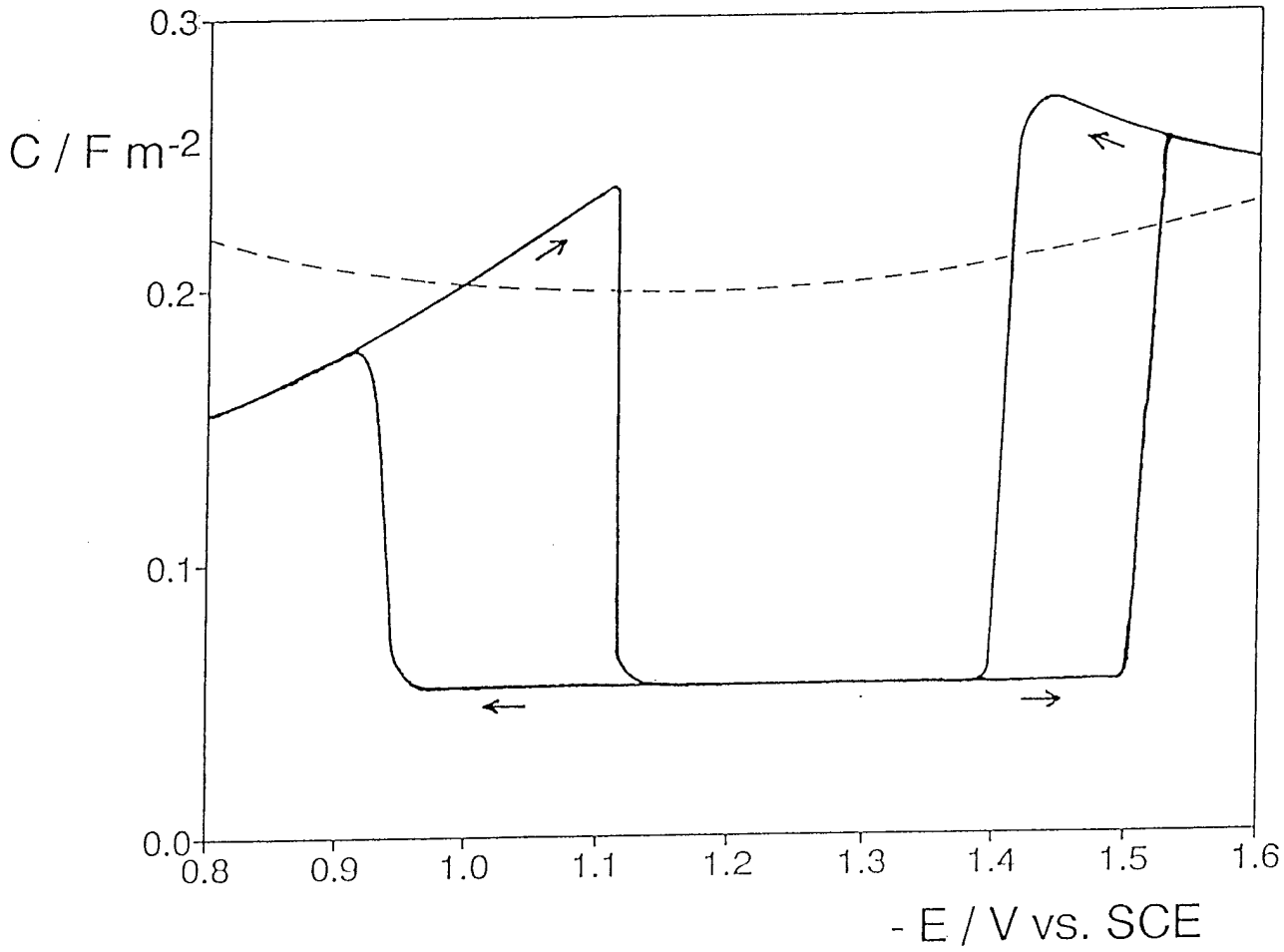

FIG. 7.

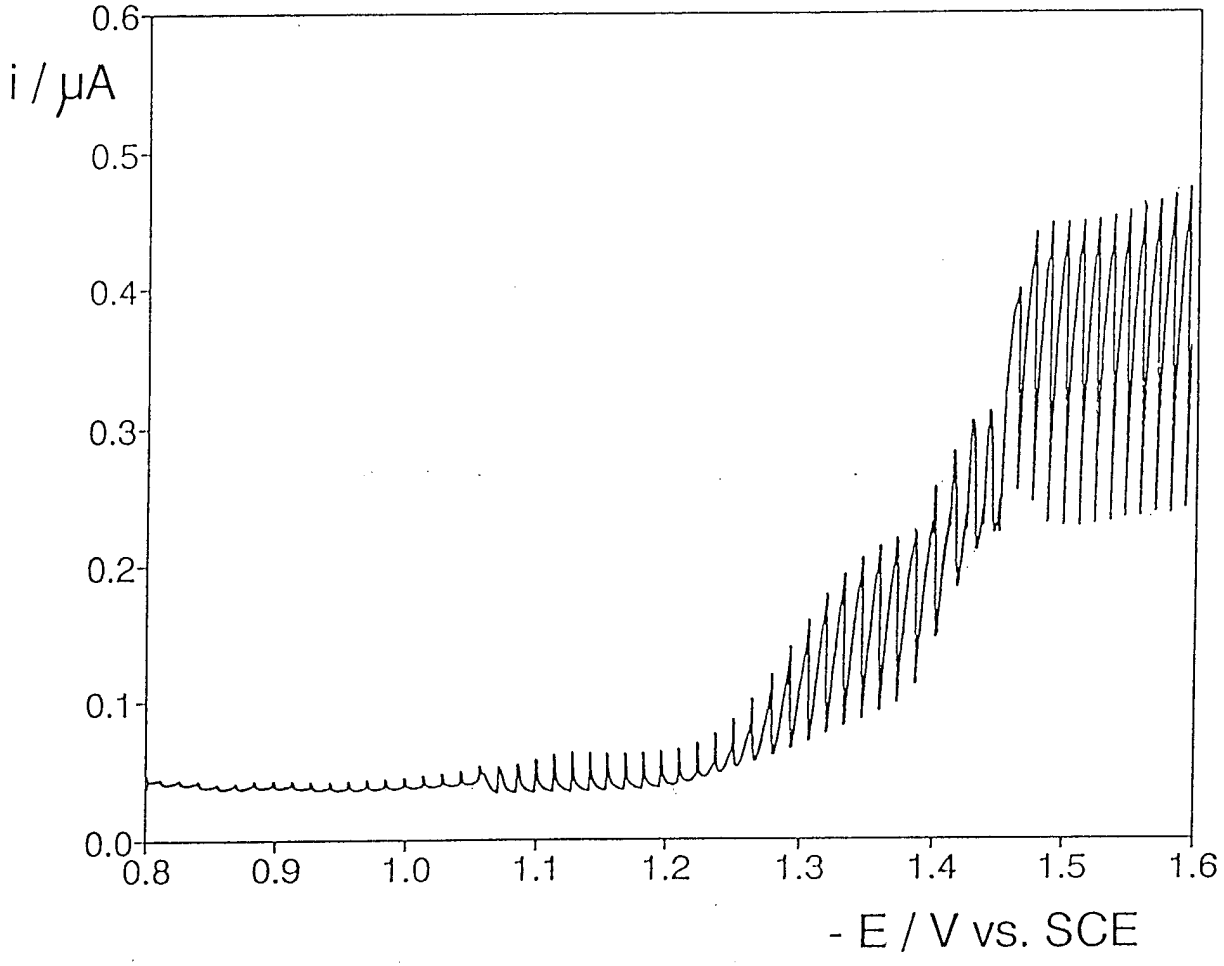

FIG. 8

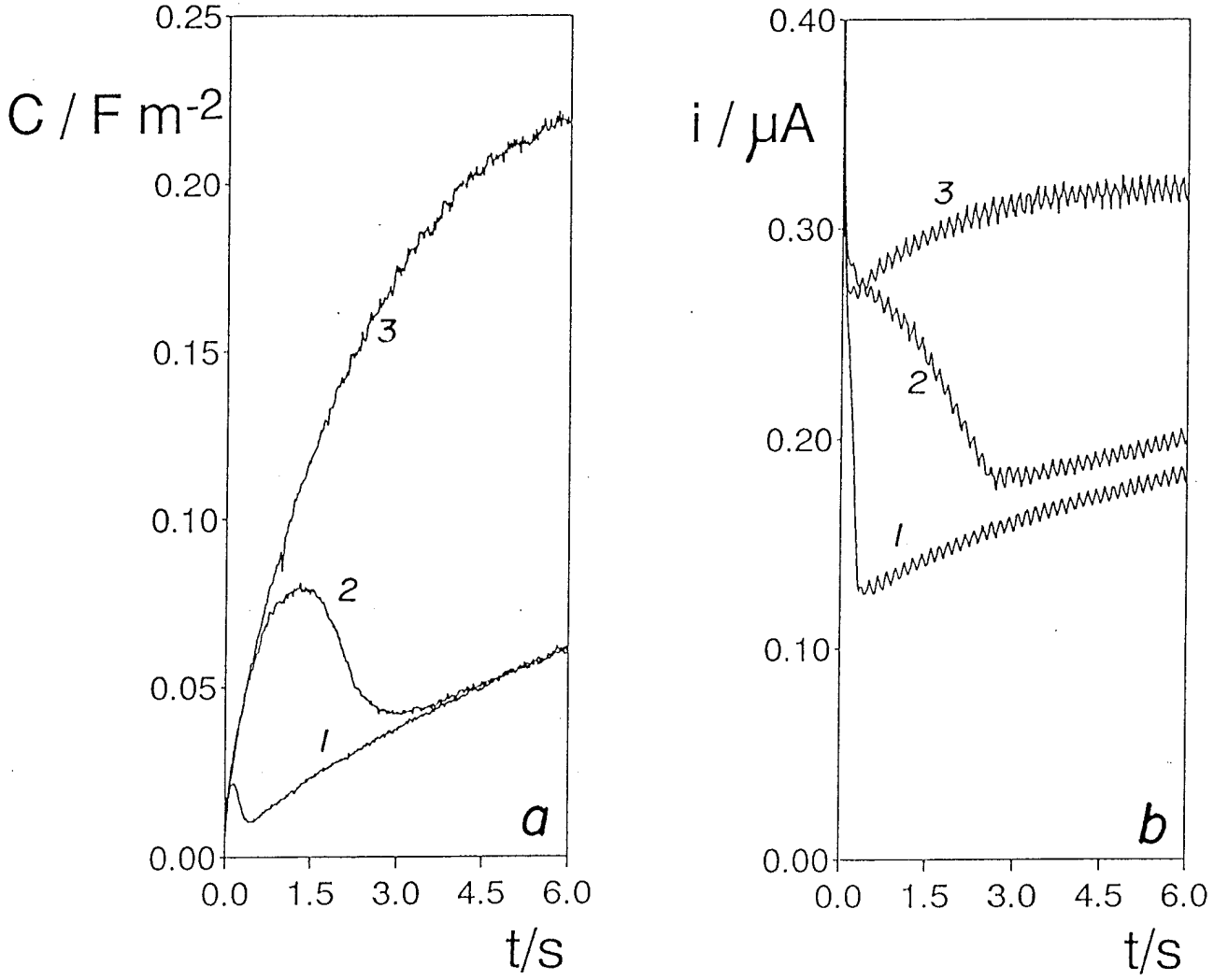
C / F m-2
0.25
0.20
0.15
0.10
0.05
0.00
0.0
1.5
3.0
4.5
6.0
t/s
3
2
1
a
i / μA
0.40
0.30
0.20
0.10
0.00
0.0
1.5
3.0
4.5
6.0
t/s
3
2
1
b

FIG. 9

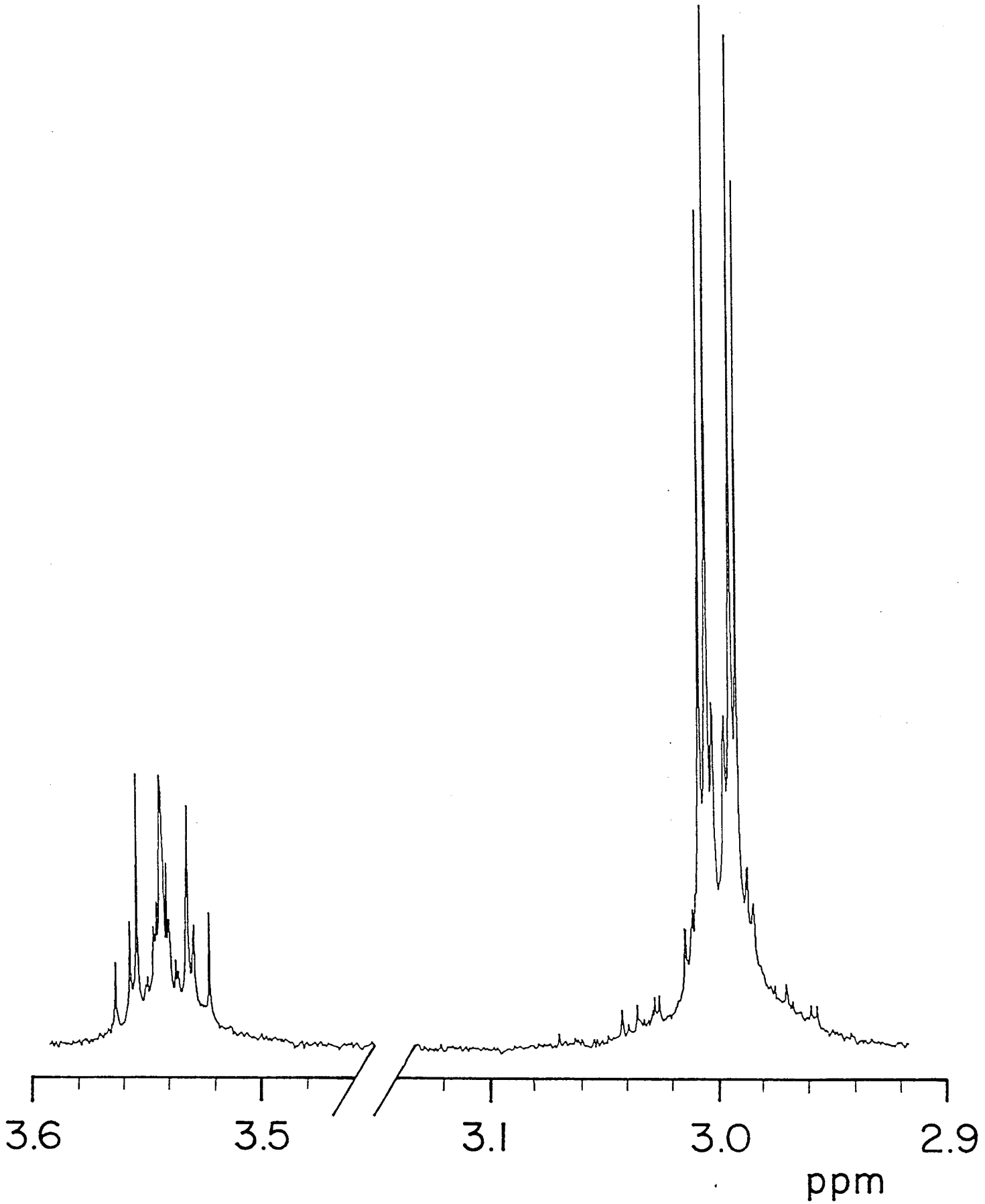

FIG. 10